Forced vibration of unevenly distributed masses
by Richard Randolph Frank

A thesis submitted to the Graduate Faculty in partial fulfillment of the requirements for the degree of
MASTER OF SCIENCE in Mechanical Engineering
Montana State University

Abstract:
Forced vibration has been used extensively in the transportation or separation of various sized particles. The forcing frequency is usually created with a rotating or reciprocating unbalance that impresses a periodic, harmonic motion. This motion is directed to impart both a horizontal and a vertical movement to the particle. This thesis shows the development of the equations, with their boundry conditions, that describe, the motion of unattached particles on a vibrating platform. Results from these theoretical equations were tabulated in table form and compared with the test results.

A high powered stroboscope was used with a photoelectric pickoff and a flash delay to photograph various stages in the cycle of rock particles on a vibrating platform. The position of the eccentric weights was used as a marker to determine the point in the vibrating platform's cycle that the photographs were taken. Various exciting frequencies and exciting forces were photographed for comparison with the theoretical results.

The photographs from the experimental tests are included in this thesis along with an explanation of their position in the cycle. A comparison with the theoretical results given in the tables showed that a very accurate and consistent relationship between thg two results existed. From these results, it has become evident that further analysis could be carried out using the stroboscope and possibly slow motion picture or multiple flash photography along with the single flash photography.

FORCED VIBRATION OF UNEVENLY DISTRIBUTED MASSES

by

RICHARD RANDOLPH FRANK

A thesis submitted to the Graduate Faculty in partial fulfillment of the requirements for the degree

of

MASTER OF SCIENCE

in

Mechanical Engineering

Approved:

H. F. Mullikan
Head, Major Department

by T. R. Murphy, Acting Head
R. C. Challender
Chairman, Examining Committee

Louis D. Smith
Dean, Graduate Division

MONTANA STATE UNIVERSITY
Bozeman, Montana

August, 1965

Acknowledgement

Special thanks and appreciation are extended to Ralph C. Challender, Associate Professor M. E. Dept., for his assistance and advice in carrying out the testing procedures and the development of this thesis. Special appreciation is also extended to David H. Drummond, Associate Professor M. E. Dept., for his assistance and advice in the design and development of the test model. Special thanks are extended to Bernard Danhof and B. T. Siefert, laboratory technicians in the M. E. Dept., who supplied many of their skills to the construction of the equipment.

Special appreciation is extended to Mr. M. G. Long for his advice and assistance in making the construction of the test model possible.

TABLE OF CONTENTS

LIST OF TABLES

LIST OF FIGURES

Abstract

Forced vibration has been used extensively in the transportation or separation of various sized particles. The forcing frequency is usually created with a rotating or reciprocating unbalance that impresses a periodic, harmonic motion. This motion is directed to impart both a horizontal and a vertical movement to the particle. This thesis shows the development of the equations, with their boundry conditions, that describe the motion of unattached particles on a vibrating platform. Results from these theoretical equations were tabulated in table form and compared with the test results.

A high powered stroboscope was used with a photoelectric pickoff and a flash delay to photograph various stages in the cycle of rock particles on a vibrating platform. The position of the eccentric weights was used as a marker to determine the point in the vibrating platform's cycle that the photographs were taken. Various exciting frequencies and exciting forces were photographed for comparison with the theoretical results.

The photographs from the experimental tests are included in this thesis along with an explanation of their position in the cycle. A comparison with the theoretical results given in the tables showed that a very accurate and consistent relationship between the two results existed. From these results, it has become evident that further analysis could be carried out using the stroboscope and possibly slow motion picture or multiple flash photography along with the single flash photography.

CHAPTER 1

INTRODUCTION

Vibration could be described as the motion of a mass under a constant change of displacement, velocity, and acceleration. If this motion is repeated over a definite interval of time it is called periodic motion. The simplest periodic motion is harmonic motion, which can be represented by a sine or cosine function.

If a vibrating system is set into motion by an external exciting force, it is said to be a forced vibration. Possibly the most common external exciting force for a vibrating system would be a reciprocating or rotating unbalance. This type of exciting force would impress a harmonic motion with a periodic frequency that would dominate the system. The forces on this system are related by Newton's second law of motion; the sum of the external forces must equal the inertia force. This is indicated by the following equation of motion for a forced vibrating system:

$$m\ddot{x} + c\dot{x} + kx = f(t)$$

where f (t) is the exciting force and m, c, and k are the mass, damping coefficient, and spring constant of the system, respectively. The displacement of the system is given by x which is assumed positive in the upward direction. The first derivitive of x with respect to time is the velocity, denoted by $\dot{x}$, and the second derivitive is the acceleration, denoted by $\ddot{x}$. The exciting force for a rotating or reciprocating unbalance, moving at a constant angular velocity, ω, may be represented by the following:

$$f(t) = F \sin \omega t = me\omega^2 \sin \omega t$$

where m is the mass of the unbalanced weights, e is the eccentricity, and t represents time.

Once a forced vibrating system reaches the steady-state oscillation a particular solution to its equation of motion may be expressed as

$$x = X \sin (\omega t - \phi)$$

where X is the amplitude of vibration and ϕ is the angle at which the displacement lags the exciting force.

Figure 1 shows the vector relationship of the forces on the system as represented by the equation of motion and its solution. From the geometry of this diagram, it may be seen that the amplitude of vibration can be represented as

$$X = \frac{F}{\sqrt{(k - m\omega^2)^2 + (c\omega)^2}}$$

Further analysis shows that this may be rewritten as

$$X = \frac{\frac{m}{M} e \left(\frac{\omega}{\omega_n}\right)^2}{\sqrt{\left[1 - \left(\frac{\omega}{\omega_n}\right)^2\right]^2 + \left[2 \zeta \frac{\omega}{\omega_n}\right]^2}}$$

Where ω_n is the natural frequency of the system and ζ is the damping factor. A plot of this equation with a very small damping factor is shown in Figure 2. When the frequency of the exciting force matches the natural frequency of the system, extremely large amplitudes result. Further study of this graph shows that as the forcing frequency approaches 4 or 5 times the natural frequency, the amplitude of the system approaches

$$X = \frac{me}{M}$$

where M is the total mass of the vibrating system.

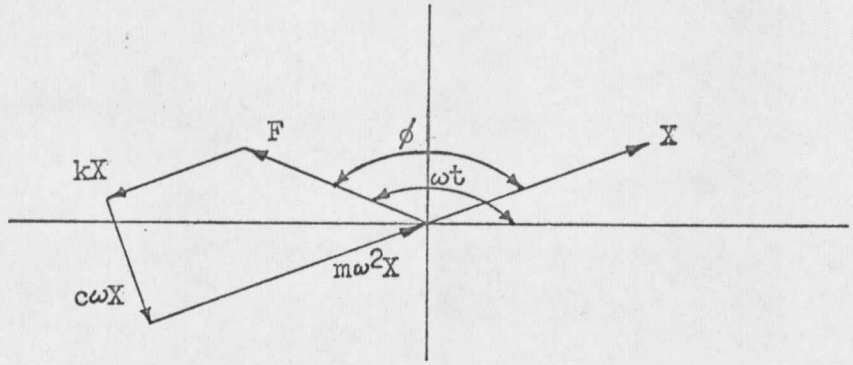

Figure 1. Vector diagram of the forces on a forced vibration system.

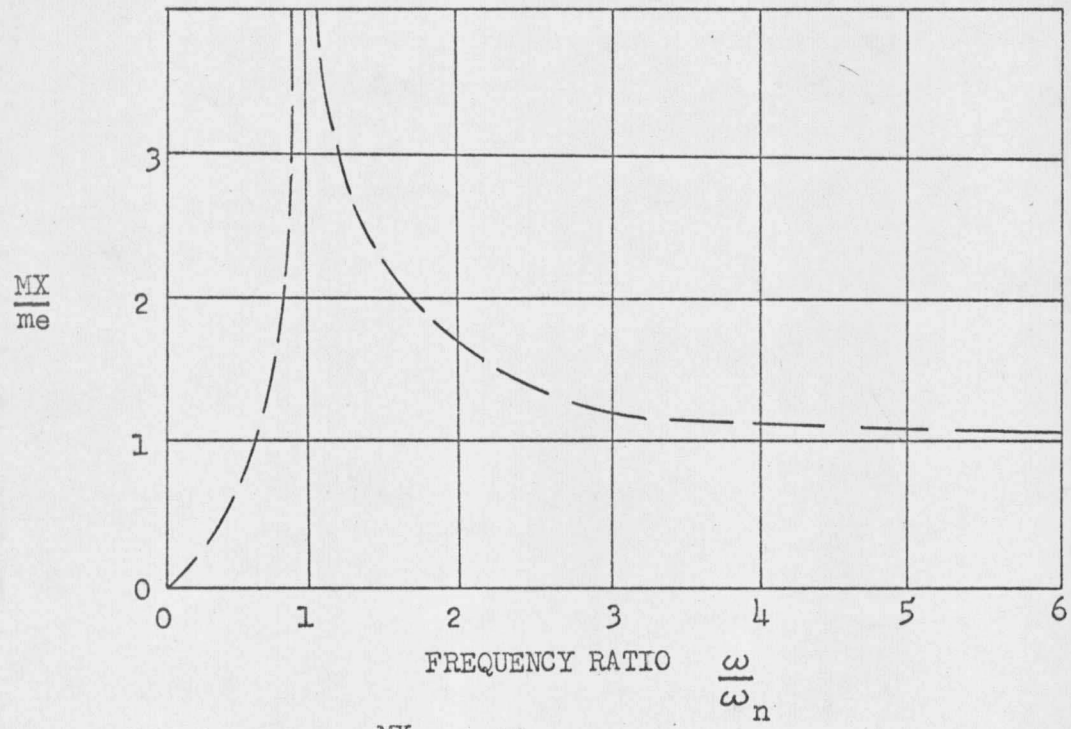

Figure 2. Plot of $\frac{MX}{me}$ vs. $\frac{\omega}{\omega_n}$ for a very small damping factor in a forced vibration.

Figure 3 shows the relationship between the frequency ratio, ω/ω_n, and the phase angle, ϕ, for a very small damping factor. When the forcing frequency approaches 4 or 5 times the natural frequency, the phase angle approaches 180 degrees. When this happens in a forced vibration, the displacement will be about 180 degrees out of phase with the exciting force.

Since the amplitude at any time, t, is represented by x, the acceleration at any time, t, is represented by

$$\ddot{x} = -\omega^2 X \sin(\omega t - \phi)$$

A graphical representation of the displacement and acceleration is shown in Figure 4. The acceleration is 180 degrees out of phase with the displacement. The equation indicates that the maximum acceleration of the vibrating system will occur when $\sin(\omega t - \phi)$ is equal to unity. This will take place each time that the maximum displacement of the vibrating unit occurs. The maximum acceleration may then be expressed as

$$\ddot{x}_{max} = \omega^2 X$$

One important use of forced vibration is the separation or transportation of large quantities of various materials. Various sized particles may be separated according to size by using a vibrating screen with openings that are large enough for the smaller particles to pass through, but too small for the larger particles. Little or no research has been done on the analysis of the motion of the particles in this type of system. The particles will act as ballistic projectiles through part of their cycle and will follow the sinusoidal motion of the screening platform through the remaining portion of their cycle. The two portions of the

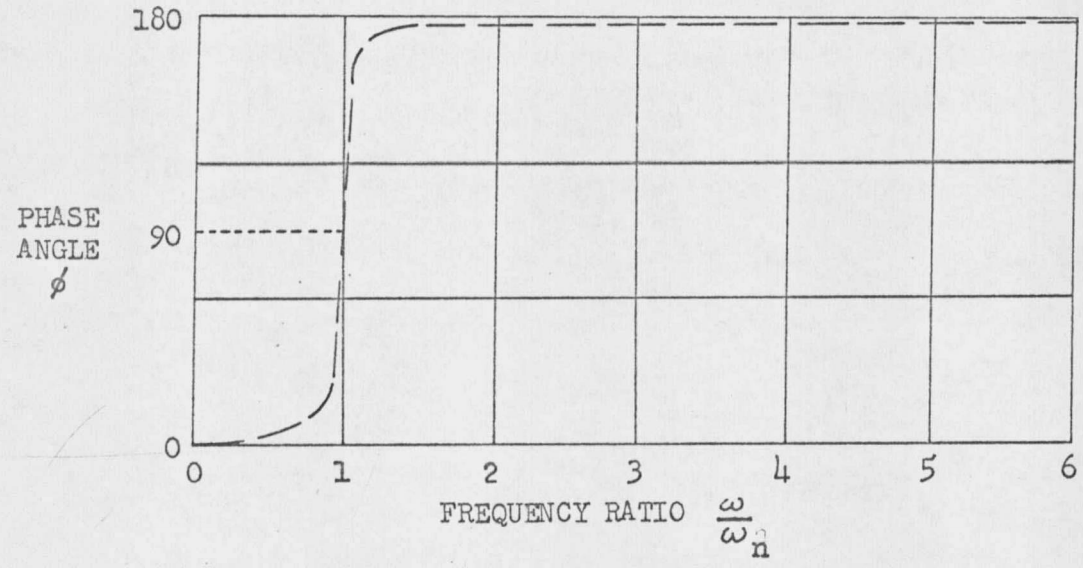

Figure 3. Plot of ϕ vs. $\frac{\omega}{\omega_n}$ for a very small damping factor in a forced vibration.

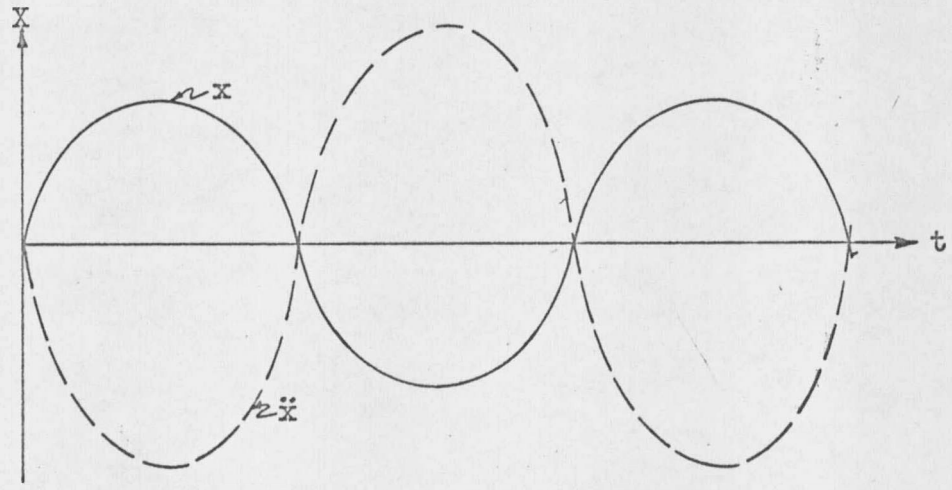

Figure 4. Plot of displacement, x, and acceleration, $\ddot{x}$, vs. time, t, in harmonic motion.

cycle must be analyzed separately and then combined to get a more accurate picture of the actual motion.

The notation used in this thesis is defined at its first appearance and is consistently used throughout the text.

CHAPTER 2

THEORETICAL DEVELOPMENT

As a preliminary analysis, consider a single particle of mass resting unattached to a platform which is set into a harmonic oscillation by an external exciting force. The motion of the particle resting on the platform would depend upon $\ddot{x}_{max}$ of the platform. If the maximum acceleration of the vibrating platform were less than or equal to the acceleration of gravity, g, the motion of the particle would be the same as the motion of the platform. As was mentioned previously, the maximum acceleration of the platform would occur at its extreme displacement positions. At the uppermost position of the platform the acceleration will be a maximum in the downward direction. If this is exactly equal to the acceleration of gravity, then the force on the particle due to the platform would be zero at that instant.

As $\ddot{x}_{max}$ is increased beyond that of g, the particle will leave the platform through part of its cycle and ride it through the remaining portion of the cycle. Figure 5 shows the relationship between the path that a particle of mass would take and that of the platform after the platform has passed the equilibrium position in its upward swing. For the conditions given in Figure 5, the particle of mass will act as a projectile for part of its cycle and will follow the motion of the screen during the remaining portion of the cycle.

If the frequency of the exciting force was such that the acceleration of the platform was exactly equal to that of gravity at time, t_1, and again at t_2, the particle would act as a projectile during this interval of time. This is shown in Figure 6. The particle will still be a projectile during the time interval between t_2 and t_3, which is the time

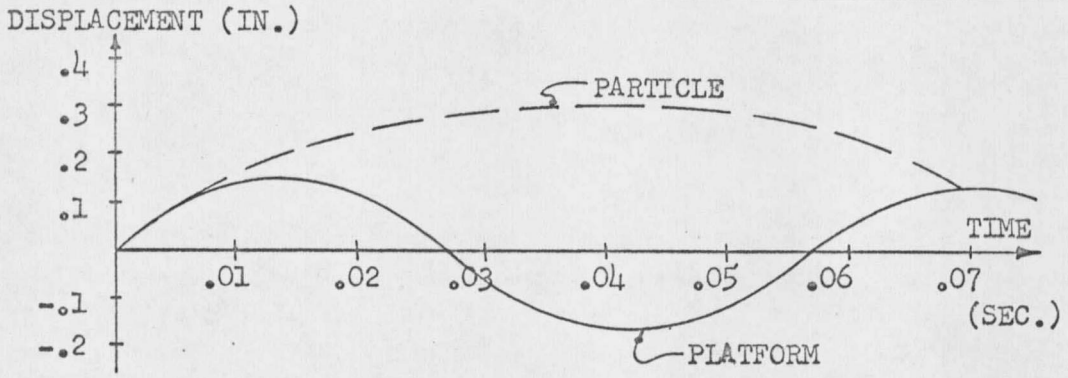

Figure 5. Verticle displacement of particle and platform vs. time. (The platform is moving vertically with an amplitude of 0.1355 in. and a frequency of 110 rad./sec.)

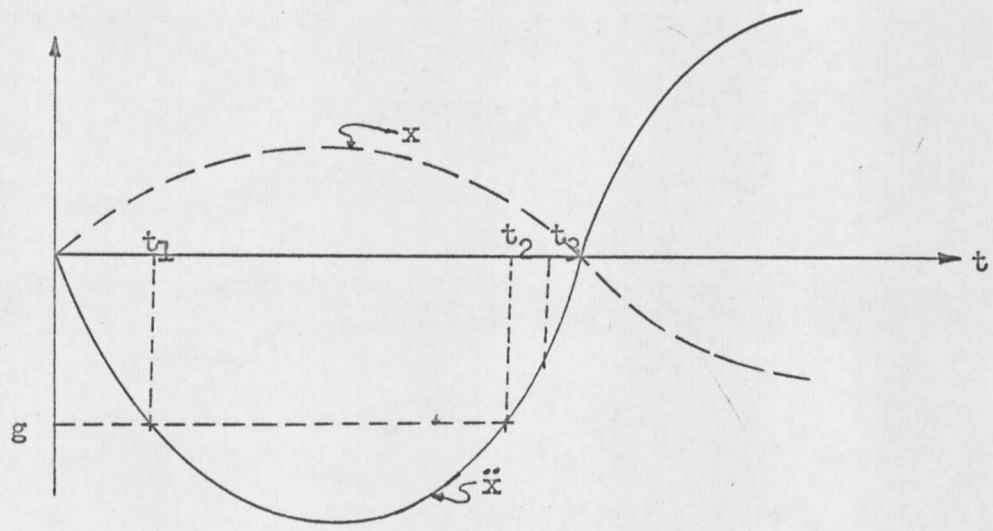

Figure 6. Plot of acceleration vs. time for a platform whose acceleration goes beyond that of gravity.

required for the particle to overtake the platform once the platform's acceleration has dropped below that of gravity. The acceleration of the particle through its cycle can be represented by the following set of equations and their boundary conditions.

$$\ddot{x} = -X\omega^2 \sin \omega t \qquad 0 \leq t \leq t_1$$

$$\ddot{x} = -g \qquad t_1 \leq t \leq t_2$$

$$\ddot{x} = -g \qquad t_2 \leq t \leq t_3$$

$$\ddot{x} = -X\omega^2 \sin \omega t \qquad t \geq t_3$$

If these equations are integrated with respect to time, a new set of equations are developed describing the particle's velocity.

$$\dot{x} = X\omega \cos \omega t + C_1 \qquad 0 \leq t \leq t_1$$

$$\dot{x} = -gt + C_2 \qquad t_1 \leq t \leq t_2$$

$$\dot{x} = -gt + C_2 \qquad t_2 \leq t \leq t_3$$

$$\dot{x} = X\omega \cos \omega t + C_1 \qquad t \geq t_3$$

In a similar manner the particles displacement at any time, t, may be developed.

$$x = X \sin \omega t + C_1 t + C_3 \qquad 0 \leq t \leq t_1$$

$$x = -gt^2/2 + C_2 t + C_4 \qquad t_1 \leq t \leq t_2$$

$$x = -gt^2/2 + C_2 t + C_4 \qquad t_2 \leq t \leq t_3$$

$$x = X \sin \omega t + C_1 t + C_3 \qquad t \geq t_3$$

Since the particle will be following the exact path of the platform between 0 and t_1, the constants C_1 and C_3 will be zero. The constants C_2 and C_4 will depend upon the values of X and ω.

These equations define only the vertical motion of the particle. A horizontal movement must also be present to transport the particle across the platform. A horizontal movement, along with the vertical displacement, is obtained by directing the vibratory motion of the platform in a direction at some angle, θ, from the horizontal. The schematic drawing in Figure 7 represents one way that this may be accomplished. Once a horizontal component of displacement is introduced, the equations for the x- direction must be multiplied by sin θ and those for the y- direction by cos θ. Since the motion of the platform in the horizontal direction is also a periodic, harmonic motion, the velocity of the particle in the horizontal direction can be represented by the following set of equations using the same boundary conditions as those used in the equations for the vertical analysis.

$$\dot{y} = X\omega \cos\theta \cos\omega t \qquad 0 \leq t \leq t_1$$

$$\dot{y} = X\omega \cos\theta \cos\omega t_1 \qquad t_1 \leq t \leq t_3$$

$$\dot{y} = X\omega \cos\theta \cos\omega t \qquad t \geq t_3$$

By integrating these velocity equations with respect to time, the set of equations describing the horizontal movement of the particle can be developed.

$$y = X \cos\theta \sin\omega t \qquad 0 \leq t \leq t_1$$

$$y = X\omega t \cos\theta \cos\omega t_1 + C_5 \qquad t_1 \leq t \leq t_3$$

$$y = X \cos\theta \sin\omega t + C_6 \qquad t \geq t_3$$

The solution of the x and y displacement of a particle will depend upon the values of X, ω, and θ. For a change in any one or more of these values, the values of the constants C_2, C_4, C_5, and C_6 will also change.

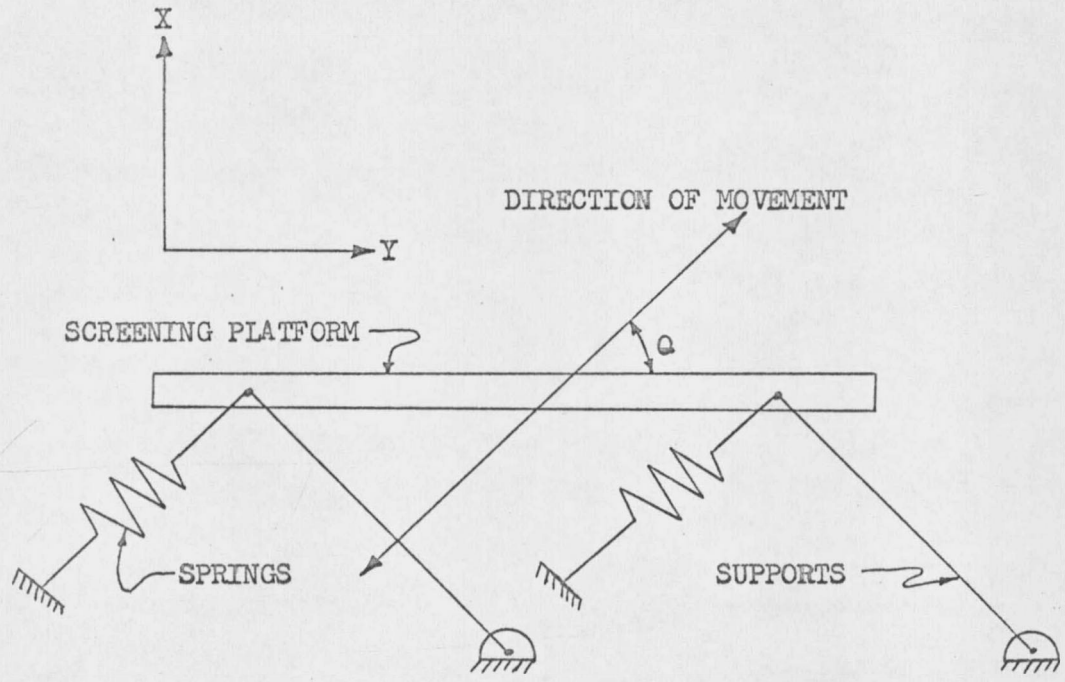

Figure 7. One method of attaining both a horizontal and a vertical component of motion. (Both components are necessary in screening operations to move the particles down the platform.)

A trial-and-error method of solution must be used to evaluate these constants for any given case. In the theoretical analysis of the test model described in Chapter 3, many different input values of X, ω, and θ were used to determine the various paths that a particle may take in its movement down the platform. The solutions to a series of these equations for various input values become extremely time consumming by the trial-and-error method. Therefore, a FORTRAN program for the 1620 Digital Computer was written to determine these values. This program is shown in Figure 8. The input values that are read into the computer are given as AM, E, D, and ATHETA. AM is the weight of the eccentric unbalance and E is the eccentricity of this weight. D is the diameter of the driving pulley on the motor used to drive the unbalanced weights. ATHETA is the angle in degrees between the direction of movement of the platform and the horizontal. This program reprints the input values for identification of the results. These values are followed by X, which is one half the maximum movement of the platform and XO which is the maximum amplitude of the platform in the vertical direction. The first value of the column headed T is the time, t_1, and the last value is the time, t_3. The remaining values are equal increments of time between these two values. The values of time are recorded from time equal zero when the platform is in the equilibrium position moving upward. The position of the particle and platform, corresponding to the values of time, is given by X and Y ROCK and X and Y SCRN, respectively. Table I through Table IV are the output for four variations to this program.

```
  1  FORMAT (4F10.0)
  2  FORMAT (5HINPUT, 4F7.2, 5X, 3H X =, F7.4, 7H  XO =, F7.4, //)
  3  FORMAT (48H    T    X ROCK    Y ROCK    X SCRN    Y SCRN)
  4  FORMAT (F8.6, 4F10.5)
 24  FORMAT (1H, ///)
 11  READ 1, AM, E D, ATHETA
     X = AM*E/(74.0 + AM) + .00005
     THETA = (ATHETA/360.) *6.2831853
     AB = X*SINF(THETA)
     W = 22.05*D
     IF(SENSE SWITCH 1) 5, 6
  5  PUNCH 2, AM, E, D, ATHETA, X, AB
     GO TO 7
  6  PRINT 2, AM, E, D, ATHETA, X, AB
  7  B = SINF (THETA)
     ALPHA = 386. / (X*W*W*B)
     IF (ALPHA - 1.) 8, 9, 9
  8  BETA = ATANF (ALPHA/ (1. - ALPHA*ALPHA)** .5)
     TA = BETA/W
     C = COSF (BETA)
     CA = X*W*B*C + 386. *TA
     GO TO 12
  9  IF (SENSE SWITCH 1) 99,999
 99  PUNCH 10
     GO TO 11
 10  FORMAT (25HINSUFFICIENT ACCELERATION, ///)
999  PRINT 10
     GO TO 11
 12  CB = X*B*SINF(BETA) + 193. *TA*TA-CA*TA
     TB = CA/386.
     TI = TB - TA
     IF(SENSE SWITCH 1) 26, 27
 26  PUNCH 3
     GO TO 25
 27  PRINT 3
 25  TB = TB + TI
 13  FT = - 193. *TB*TB + CA*TB + CB - X*B*SINF(W*TB)
     IF(ABSF(FT) - .000001)15, 15, 28
 28  IF(FT) 14, 15, 25
 14  TI = TI/2
     TB = TB - TI
     GO TO 13
 15 GAMMA = COSF (THETA)
```

Figure 8. Digital Computer Program

```
      CY = X*GAMMA*SINF(BETA) - X*BETA*GAMMA*C
      TI = (TB - TA) /9.
      T = TA
      K = 1
16    XS = - 193. *T*T + CA*T + CB + .000005
      YS = X*W*T*GAMMA*C +CY + .000005
      TS = T + .000005
      XL = AB*SINF(W*T) + .000005
      YL = X*GAMMA*SINF(W*T) + .000005
      IF(SENSE SWITCH 1) 17, 18
17    PUNCH 4, TS, XS, YS, XL, YL
      GO TO 19
18    PRINT 4, TS, XS, YX, XL, YL
19    IF (K - 10) 20, 21, 21
20    K = K + 1
      T = T + TI
      GO TO 16
21    IF (SENSE SWITCH 1) 22, 23
22    PUNCH 24
      GO TO 11
23    PRINT 24
      GO TO 11
      END
```

Figure 8. (Continued)

CHAPTER 3

DESIGN AND CONSTRUCTION OF TEST MODEL

A small vibrating screen was constructed as a laboratory test model. The model, which is shown in Figure 9, was designed with as many variable parameters as possible. These parameters include frequency, amplitude, exciting force, angle of throw, and a means to vary the quantity of flow onto the vibrating screen.

In this model, as in any forced vibration, the frequency of the system is controlled by the frequency of the exciting force. The exciting force for this model is a rotating unbalance consisting of two 8 3/16 inch discs with weights attached. The speed of this rotating unbalance will determine the frequency of the system. A 220 volt, constant speed, alternating current motor is used to drive the unbalanced disc through a belt drive as shown in Figure 10. The motor has a speed of 1725 rpm and a power rating of 3/4 hp. Various pulley sizes are available to vary the speed of the unbalance, thus giving a variation in the forcing frequency and the exciting force.

The amplitude of the system is controlled by changing the size of the unbalanced weights or changing the eccentricity of the unbalance. A series of holes were drilled in the unbalance discs (see Figure 10) so that the weights could be relocated. Changing the weights or eccentricity will vary both the magnitude of the exciting force and the amplitude of vibration.

The entire system is mounted on four, matched leaf springs. These springs, along with the mass of the entire system, determine the natural frequency. They are mounted as cantilever beams onto the base and allowed

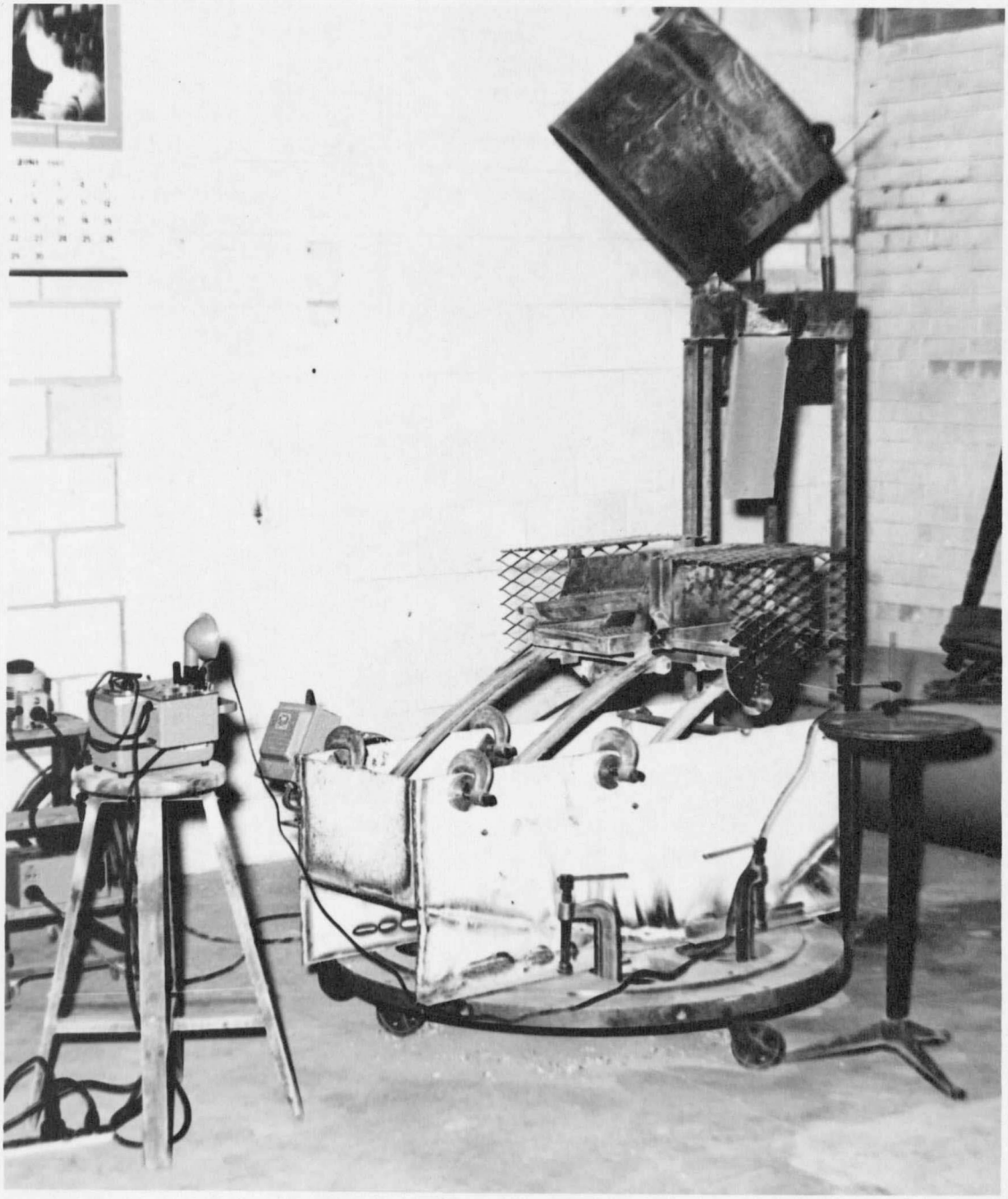

Figure 9. Experimental test model.

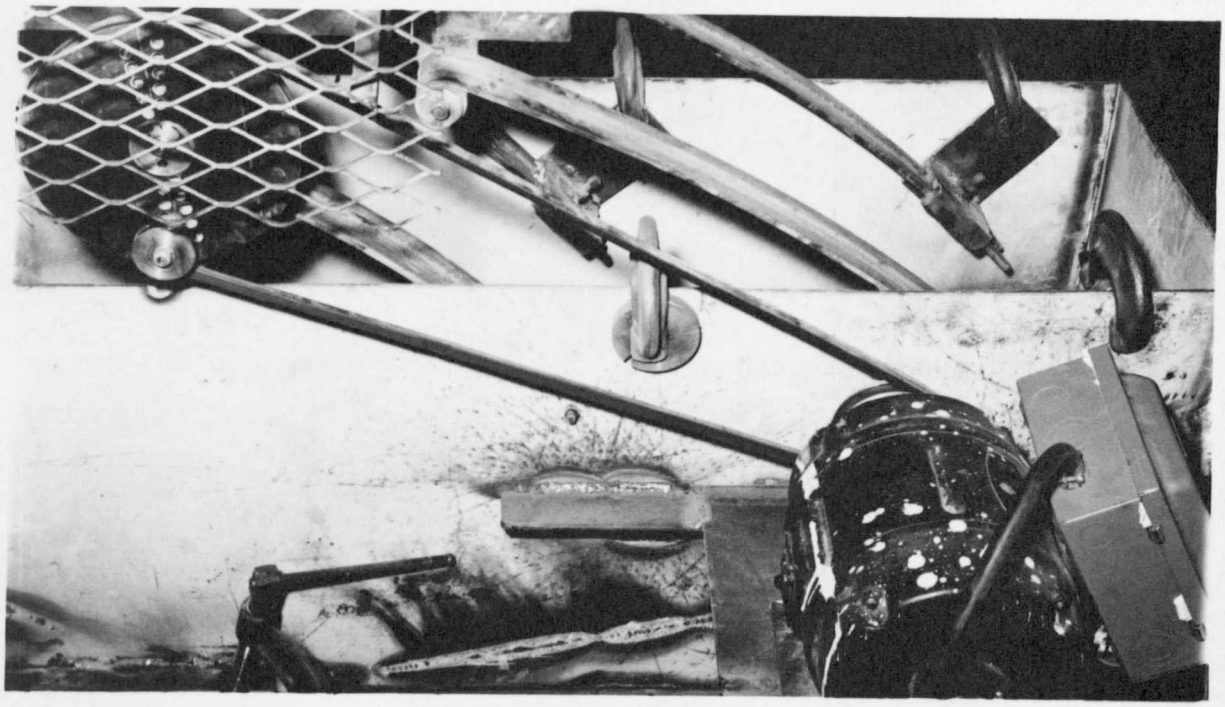

Figure 10. Eccentric unbalance drive.

Figure 11. Turntable feed mechanism.

to pivot through a pin connection at the frame of the vibrating unit as shown in Figure 10. The four leaf springs act as supports for the vibrating unit and eliminate the need for an additional pair of counter-rotating unbalanced discs to create a unidirectional exciting force. The springs can be rotated about the base through an arc of approximately 60 degrees to vary the angle of throw. The angle of throw determines the vertical and horizontal movement of the particles during each cycle of vibration.

The quantity of flow onto the screen is controlled by a turntable (see Figure 11) with a scraper blade. The turntable is driven by a direct current motor through a 48 to 1 speed reducer. A variac and two full-wave bridge rectifiers are used to control the speed of the motor. By varying the speed of the turntable a variable rate of flow is achieved. The platform was constructed using a screen with a 1/4 inch square opening using 1/8 inch wire. A crushed rock mixture of approximately 30 per cent passing through the screen was selected for the experimental analysis.

CHAPTER 4

TESTING PROCEDURES AND EQUIPMENT

The method of approach utilized in conducting the experimental analysis of the motion of the particles was the attempt to photograph the position of the rock particles relative to the platform at various stages of the cycle. Several different magnitudes of exciting force and forcing frequencies were used.

Before the photographic approach was attempted, the author ran a variety of tests, varying as many parameters as possible, in an attempt to find the two extremes in separation efficiency. This approach proved to be of little significance because of the small difference that was recorded. These results were partially due to the limited capacity of the test model.

Special instuments for stop-motion photography are required when objects in motion at a high vibrational frequency are to be photographed at a particular point in their cycle. The combination of instruments used by the author were the type 1531-A Strobotac, Electronic Stroboscope; the type 1531-P2 Flash Delay; and the type 1536-A Photoelectric Pickoff.

The Photoelectric Pickoff consists of a pickoff head with a light source and a photocell. The pickoff head is placed near a rotating object with a single shiny spot that reflects the light source back to the photocell. This produces electrical pulses which are applied to the input of the Flash Delay. The Flash Delay then synchronizes the Strobotac by inserting a controlled delay period between the trigger pulse and the resulting light flash. Therefore, by varying the delay period, the flash may be synchronized with any point in the cycle.

The photographs shown in Figure 15 through Figure 18 were taken using Eastman Tri-X film at a camera distance of 3 feet and lens setting of f/4.5. The camera was positioned at approximately 20 degrees to one side of the direction of flow of the rocks. The strobotac was placed about 3 feet from and perpendicular to the disposal edge of the screening platform as shown in Figure 12. This eliminated shadows from the retaining walls. The strobotac was set at the high intensity external input range for a single flash of 3.0 microseconds duration. This flash duration is measured at 1/3 peak intensity, where the peak light intensity at this setting is 7.0 million beam candlepower. The range switch on the Flash Delay was set on Range 2, which gives a controllable time-delay ranging from 1 millisecond to 100 milliseconds. A small piece of highly reflective tape was placed about 1.5 inches from the center of one of the unbalanced discs. The pickoff head of the Photoelectric Pickoff was placed about 2.5 inches from the rotating disc.

The photography was done during darkness to eliminate the problems involved in synchronizing the camera and Strobotac. The procedure was to hold the camera shutter open and flash the Strobotac at the desired point in the cycle. Figure 13 shows the screening platform from the approximate angle that the experimental photographs were taken.

The exciting frequencies in all of the photographic tests were well beyond that of the natural frequency of the fundamental mode of the system. This means, as was mentioned previously, that the displacement lags the exciting force by 180 degrees. The unbalanced weights would then be in their extreme upward position when the screening

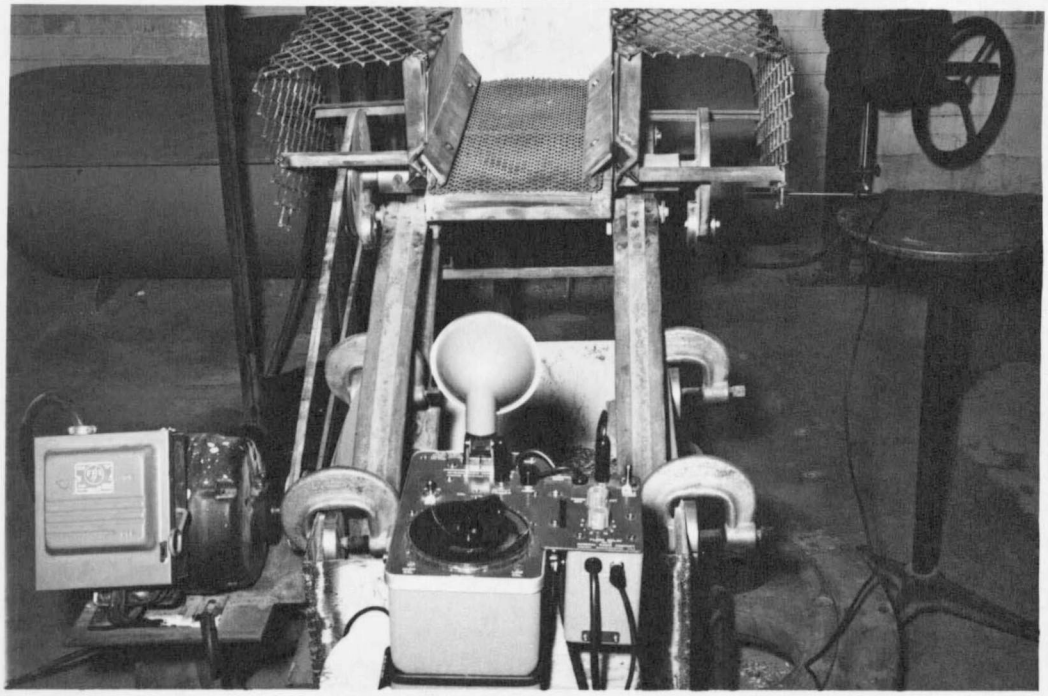

Figure 12. Strobotac position.

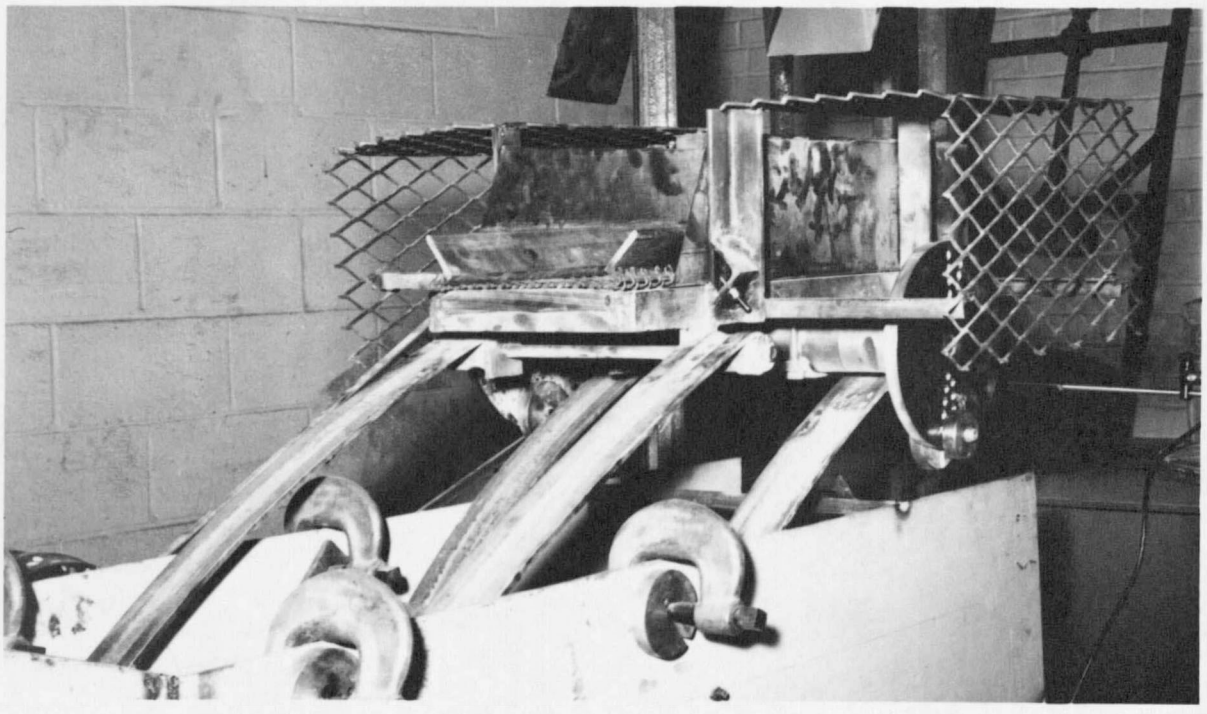

Figure 13. Camera angle for experimental photographs.

platform was at its lowermost position. The position of the unbalanced weights was used as a marker in selecting the desired point in the cycle for photographing. Eight photographs were taken with about 45 degree intervals between the unbalanced weight positions. These eight positions are shown in Figure 14. The position numbered 1 is the zero time position for the theoretical values given in Table I through Table IV.

Four, five, and six inch drive pulley sizes were used for the photographic tests. The exciting frequencies using these three pulley sizes are 88, 110, and 132 rad./sec., respectively. The period in each case may be calculated and the time from the zero time position may be determined for each photograph. At 88 rad./sec., the eccentric weight will move 45 degrees in about 0.009 sec.; at 110 rad./sec., the time required is about 0.0072 sec.; and at 132 rad./sec., only about 0.006 sec. is required.

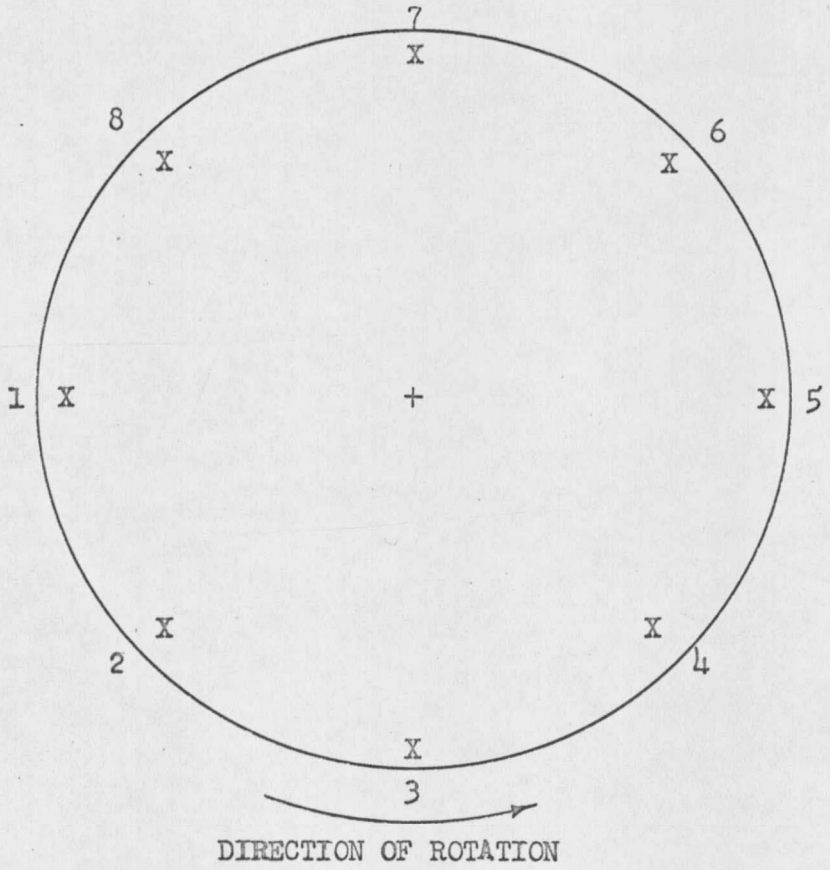

Figure 14. Eccentric weight positions.

CHAPTER 5

SUMMARY

The theoretical development in Chapter 2 leads to the results given in Table I through Table IV. These results were obtained from the theoretical equations using the FORTRAN program given in Figure 8. A wide variety of results were obtained using this program by varying the input data. The results given in the tables were examined more closely by photographing various stages in the cycle. The resulting photographs, along with their corresponding table of theoretical results, shall now be examined.

The photographs shown in Figure 15 were taken when the test model was set for an angle of throw of 57 degrees; the eccentric weights were at a distance of 3.5 inches with a total weight of 3 pounds; and the drive pulley diameter was 4 inches. These settings correspond to the input values given in Table I.

The photograph in Figure 15a shows the position of the platform and rock just as the platform passes through its equilibrium position on its upward swing. This is the number 1 position in Figure 14 and shall be considered the zero time position throughout this chapter. The numbered positions by each photograph are for the eccentric weight and indicates those shown in Figure 14. In b the platform is at its maximum positive amplitude position. The eccentric weight is in the number 3 position. This is its position at approximately 0.018 second after it has passed the zero time position. This is fairly consistent with Table I which shows the maximum positive amplitude position to occur at about 0.018 sec. The separation between the rocks and the platform becomes

Table I

Theoretical rock-screen positions for ω equaling 88 rad./sec.

INPUT 3.00 3.50 4.00 57.00 X = 0.1364 XO = 0.1144

T sec.	X ROCK in.	Y ROCK in.	X SCRN in.	Y SCRN in.
.005086	.04962	.03222	.04962	.03222
.011547	.10030	.07037	.09739	.06325
.018008	.13488	.10852	.11439	.07428
.024468	.15334	.14666	.09524	.06185
.030929	.15569	.18481	.04599	.02986
.037390	.14193	.22296	-.01779	-.01155
.043850	.11206	.26111	-.07594	-.04931
.050311	.06607	.29925	-.11010	-.07150
.056772	.00397	.33740	-.10946	-.07108
.063232	-.07422	.37555	-.07422	-.04820

Table II

Theoretical rock-screen positions for ω equaling 110 rad./sec. and E equaling 3 in.

INPUT 3.00 3.00 5.00 57.00 X = 0.1169 XO = 0.0980

T sec.	X ROCK in.	Y ROCK in.	X SCRN in.	Y SCRN in.
.002991	.03176	.02062	.03176	.02062
.009101	.08705	.06121	.08270	.05371
.015211	.12794	.10180	.09752	.06333
.021321	.15442	.14239	.06973	.04528
.027430	.16648	.18298	.01148	.00746
.033540	.16414	.22356	-.05177	-.03362
.039650	.14739	.26415	-.09241	-.06001
.045760	.11623	.30474	-.09268	-.06081
.051870	.07066	.34533	-.05246	-.03406
.057980	.01068	.38592	.01068	.00693

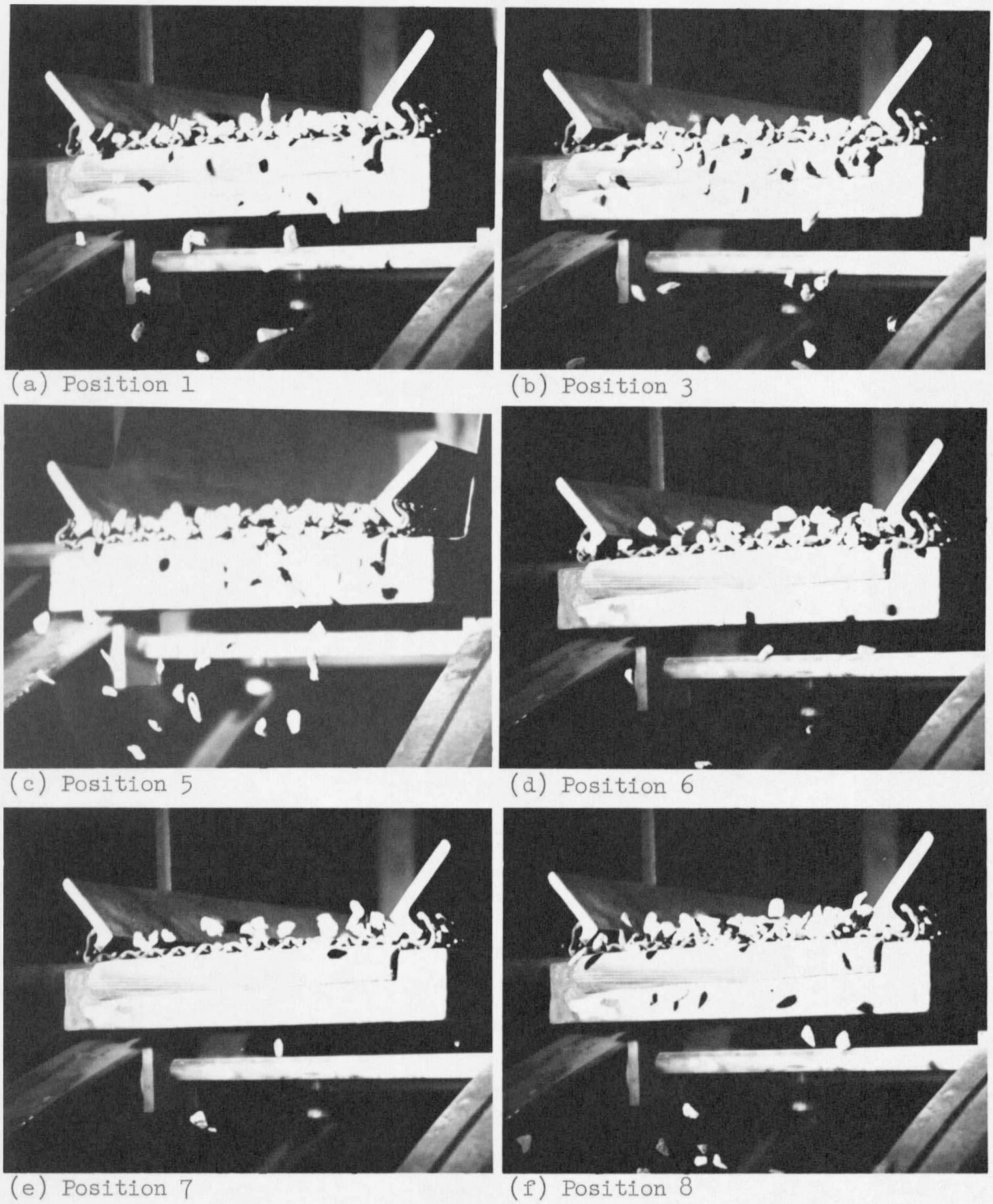

(a) Position 1 (b) Position 3

(c) Position 5 (d) Position 6

(e) Position 7 (f) Position 8

Figure 15. Rock-screen positions during one cycle for ω equaling 88 rad./sec.

more apparent in c and is a maximum in d at approximately 0.045 sec. after zero time. The maximum theoretical difference from Table I occurs at approximately 0.044 sec. The platform reaches its maximum negative position in e at approximately 0.054 sec. after zero time. The theoretical values in Table I show that the maximum negative position occurs between 0.050 and 0.056 sec. The rocks and platform are just about to come into contact in f to complete the projectile portion of the cycle at about 0.063 sec.

The test model setting for the photographs in Figure 16 correspond to the input values given in Table II. By comparing the first time value in Table I with that in Table II, it may be seen that the time required to start a separation between the rocks and the platform is almost double for the slower forcing frequency. Table II also shows that the platform has gone through more than one complete cycle before the rocks complete the projectile portion of their cycle. Figure 16a represents the zero time position. At about 0.0144 sec. after zero time the platform has reached its maximum positive amplitude in b. The theoretical value in Table II indicates that the maximum positive amplitude occurs at about 0.015 sec. In c, the platform is starting the negative portion of its cycle where a definite separation between the rocks and the platform can be readily seen. The maximum difference in separation will occur between d and e, where e is the maximum negative position of the platform. The projectile cycle is completed in f where the rocks and platform come into contact in the positive portion of the platforms cycle.

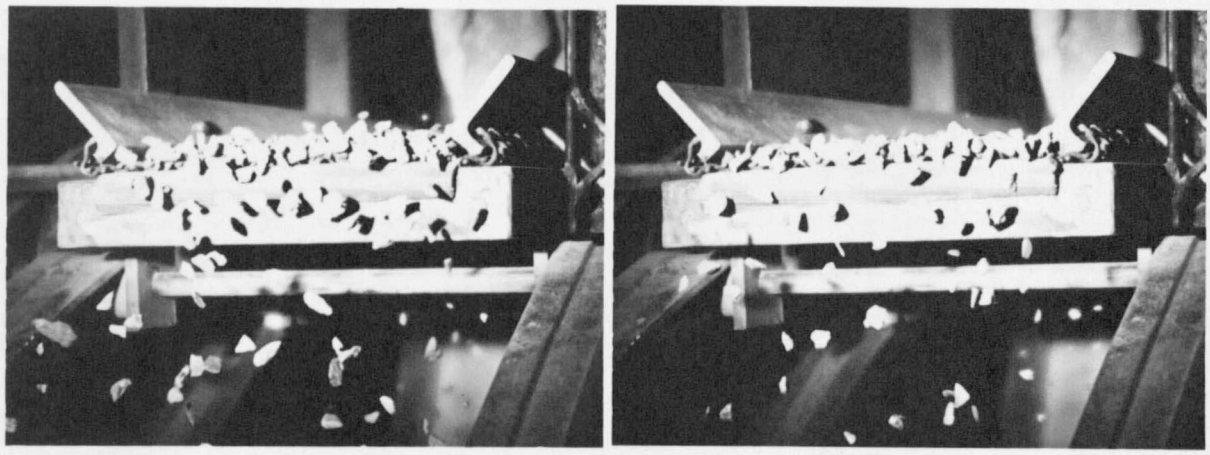

(a) Position 1

(b) Position3

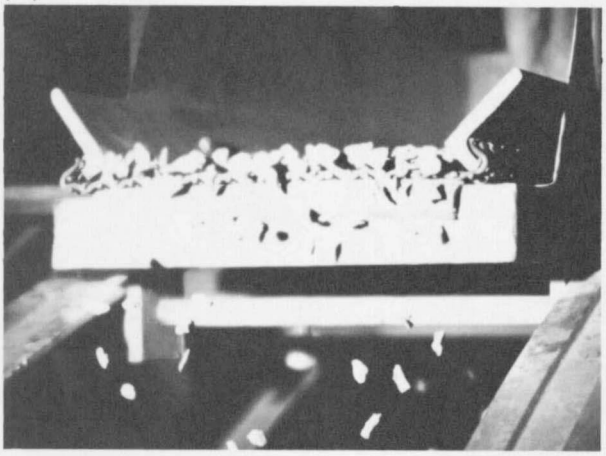

(c) Position 5

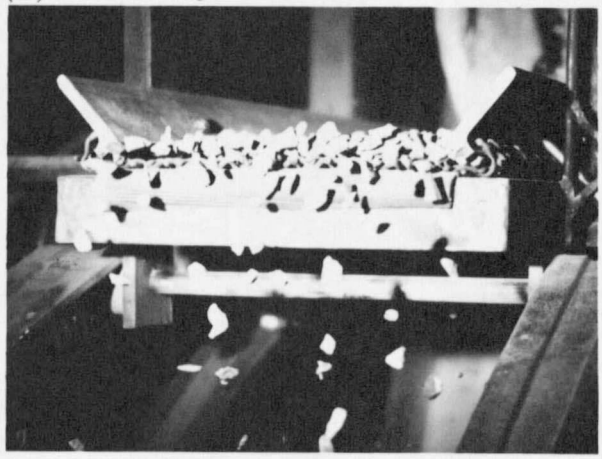

(d) Position 6

(e) Position 7

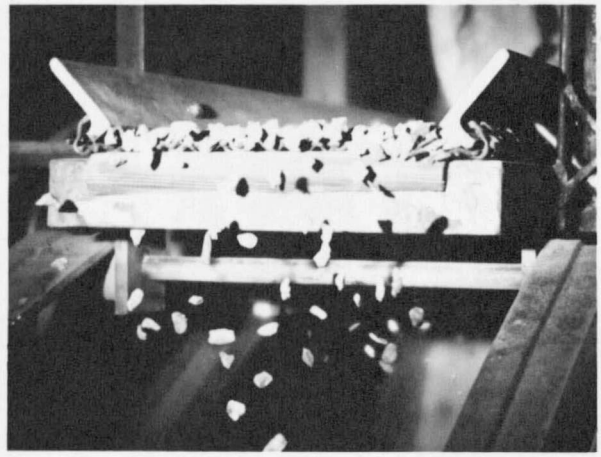

(f) Position 2

Figure 16. Rock-screen positions during one cycle for ω equaling 110 rad./sec. and E equaling 3 in.

The photographs in Figure 17 were taken with the test model at the same setting as those in Figure 16. with the exception of a half inch increase in the eccentricity. The values in Table III are the theoretical values for this setting. Since the magnitude of the exciting force is increased, the amplitude of both the rocks and the platform is increased and the time duration from zero time to the initial separation is decreased. The platform is passing through the zero time position in a. It can be seen from the photograph that the rocks are slightly above the screening platform. This indicates that the previous cycle has not yet been completed. Table III shows the position of the platform to be over half way to its peak positive amplitude at the time of impact. The platform is at its peak positive position in b where a separation of about 0.04 in. should exist. The platform is passing through its equilibrium position on its downward swing in c and is at its maximum negative position in d where the maximum separation also occurs. This maximum negative displacement occurs at about 0.0432 sec. after zero time. From Table III, the theoretical value for the maximum negative displacement will occur at about 0.043 sec. The platform is beginning its return to the positive portion of its cycle in e and has completed the projectile portion of the cycle in f at about 0.0648 sec. The theoretical completion of this portion of the cycle occurs at about 0.0625 sec.

The photographs in Figure 18 were taken with the machine set at the input values in Table IV. This forcing frequency was the fastest frequency used for the test photographs. By observing the platform with the aid of the Strobotac, a rotating motion of the platform was discovered. This

Table III

Theoretical rock-screen positions for ω equaling 110 rad./sec. and equaling 3.5 in.

INPUT 3.00 3.50 5.00 57.00 X = 0.1364 XO = 0.1144

T sec.	X ROCK in.	Y ROCK in.	X SCRN in.	Y SCRN in.
.002551	.03176	.02062	.03176	.02062
.009208	.10387	.7301	.09720	.06312
.015866	.15888	.12540	.11259	.07312
.022523	.19678	.17779	.07000	.04546
.029180	.21758	.23017	-.00862	-.00560
.035837	.22127	.28256	-.08281	-.05377
.042495	.20785	.33495	-.11435	-.07426
.049152	.17732	.38734	-.08700	-.05650
.055809	.12969	.43972	-.01485	-.00964
.062466	.06495	.49211	.06495	.04218

Table IV

Theoretical rock-screen positions for ω equaling 132 rad./sec.

INPUT 2.00 3.00 6.00 57.00 X = 0.0789 XO = 0.0662

T sec.	X ROCK in.	Y ROCK in.	X SCRN in.	Y SCRN in.
.002565	.02205	.01432	.02205	.01432
.007581	.05865	.04124	.05585	.03627
.012596	.08555	.06817	.06595	.04283
.017612	.10273	.09509	.04806	.03121
.022628	.11019	.12201	.00977	.00634
.027644	.10795	.14893	-.03266	-.02121
.032659	.09600	.17586	-.06123	-.03976
.037675	.07434	.20278	-.06381	-.04143
.042691	.04296	.22970	-.03930	-.02552
.047706	.00188	.25662	.00188	.00122

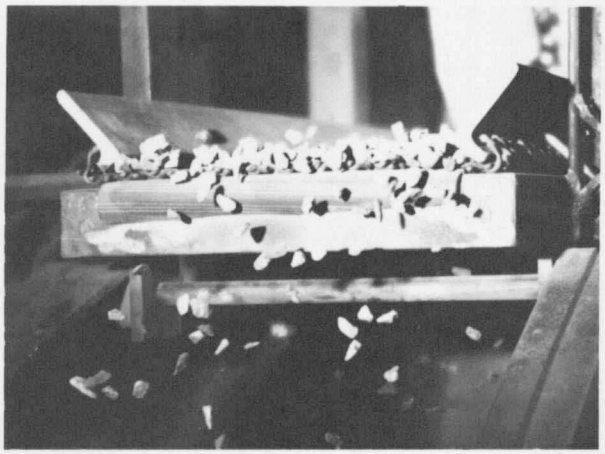

(a) Position 1

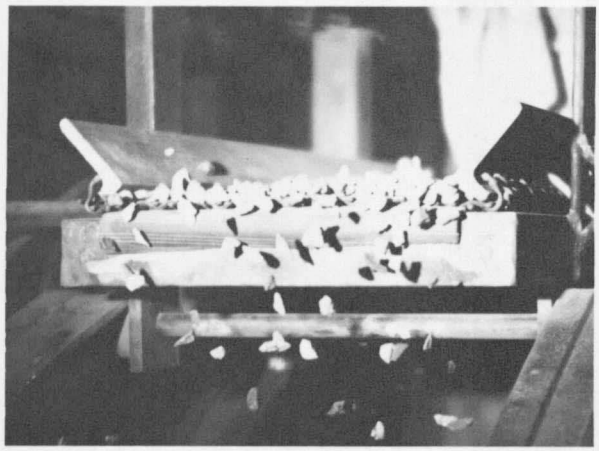

(b) Position 3

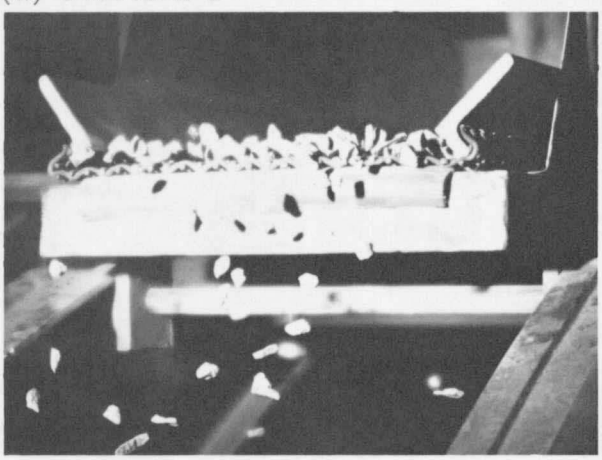

(c) Position 5

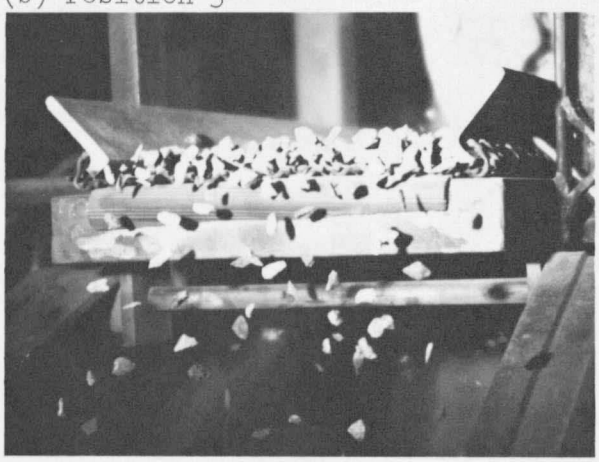

(d) Position 7

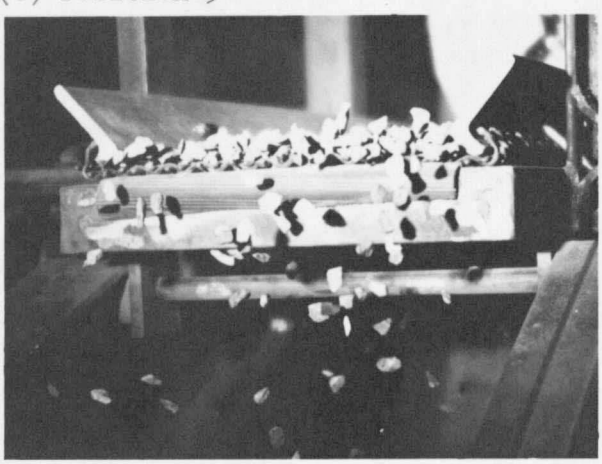

(e) Position 8

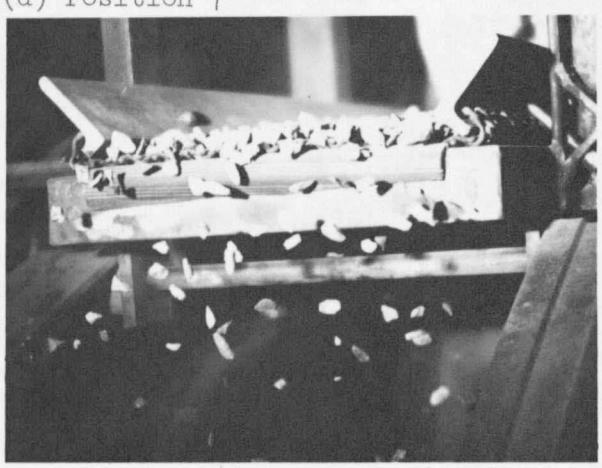

(f) Position 2

Figure 17. Rock-screen positions during one cycle for ω equaling 110 rad./sec. and E equaling 3.5 in.

indicated that the system became much more complex by introducing a second degree of freedom. The photographs in Figure 18 show particles of rock with comparatively large amplitudes. These large amplitudes were probably the result of this second degree of freedom. If these large amplitudes were ignored, a comparison with Table IV may be made. The photograph in 18a shows the rock-platform position at about 0.006 sec. after zero time. The maximum positive amplitude of the platform is shown in b and the maximun separation in c at 0.030 sec. after zero time. The maximum negative position of the platform is shown in d at 0.036 sec. after zero time. Table IV indicates that the theoretical time for the maximum negative position of the platform is about 0.036 sec. The platform is starting its upward swing in e and has come into contact with the particles in f at 0.048 sec. after zero time. The position in f is the zero time position which indicates that the platform completes one cycle each time that the rocks complete one cycle.

The foregoing analysis demonstrated the close relationship between the theoretical and actual results. Changes in the forcing frequency changed the duration of the projectile cycle and the point of impact in the platform's cycle. Changing the magnitude of the exciting force affected the amplitude of the rocks which is related to the projectile cycle and the point of impact. In all cases, the times involved were extremely small and the photographic results were remarkably consistent.

This thesis has demonstrated that any future research utilizing the stroboscope and any number of different photographic approaches along with

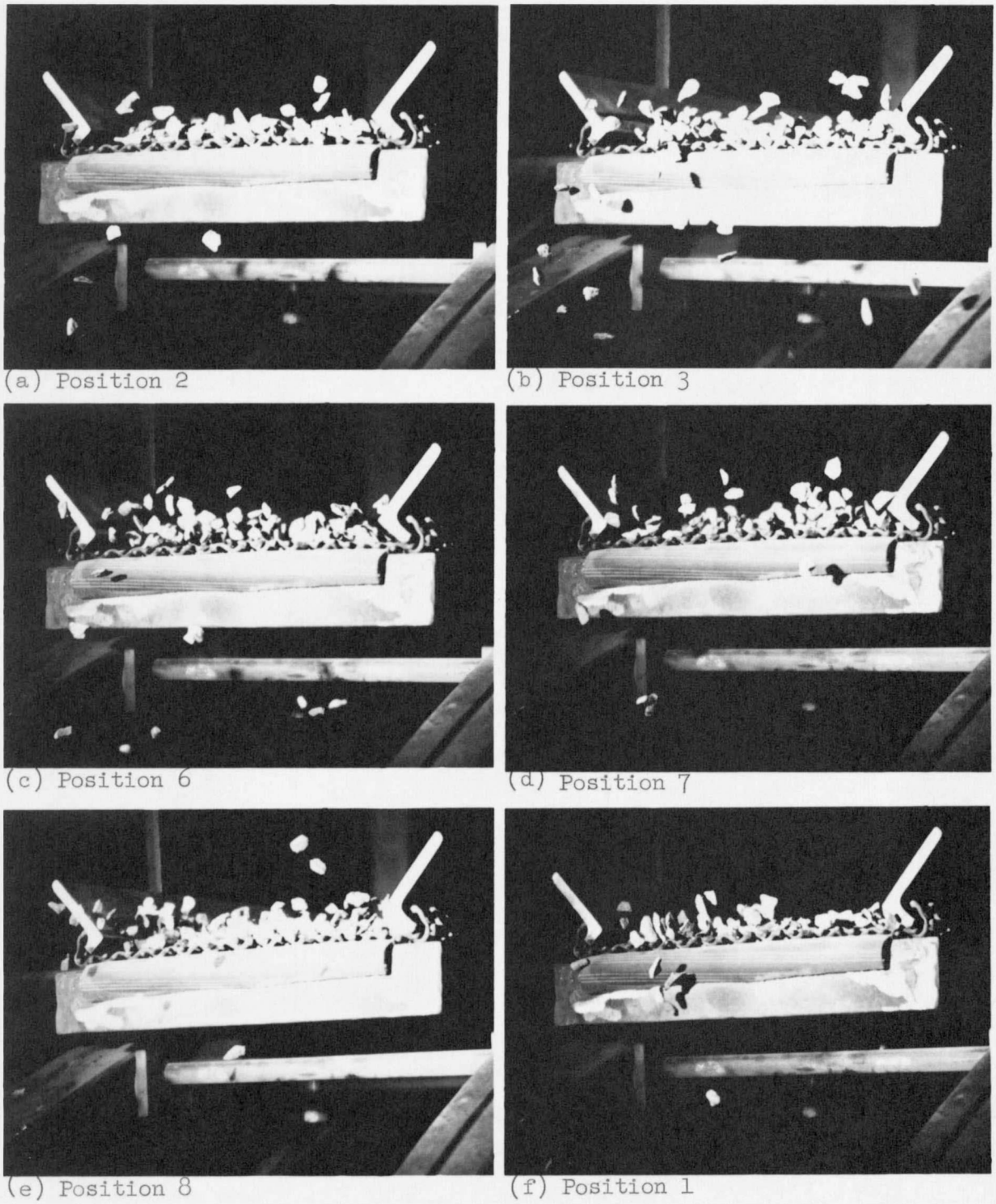

(a) Position 2 (b) Position 3

(c) Position 6 (d) Position 7

(e) Position 8 (f) Position 1

Figure 18. Rock-screen positions during one cycle for ω equaling 132 rad./sec.

the single flash photography would be highly fruitful. Two suggested photographic approaches would be multiple flash photography and slow motion picture photography.

The close relationship between the theoretical and experimental results in this thesis has demonstrated that theoretical equations may be written to closely approximate the actual motion of unevenly distributed particles on a vibrating platform. Although no practical applications may be obtained as a direct result of this thesis, the theoretical-experimental relationships shown to exist may be utilized in future research toward this goal.

The author suggests a more basic approach for future research by eliminating the uncontrollable parameters introduced by the crushed rock. This may be accomplished by making initial tests using spherical particles. Subsequent tests could increase the complexity of the particle shape to include cubes and octahedrons. Along with variations in shape, variations in specific gravity might also produce fruitful results. The screening platform may be idealized by placing a layer of sheet metal below the wire mesh. This would still retain some of the effect that the wire would have upon the particles. It may also be desirable to use a flat, smooth platform for the initial tests.

APPENDIX

LITERATURE CONSULTED

Gluck, Samuel E. "Vibrating Screens," Chemical Engineering. February 15, 1965, pp. 151-168.

Macduff, John N., and John R. Curreri. Vibration Control. New York, 1958.

Thompson, William T. Mechanical Vibrations. Englewood Cliffs, N. J., 1963.

Handbook of High-Speed Photography, General Radio Company, West Concord, Mass., 1963.

"Materials Handling and Processing Equipment," Link-Belt, Catalog 1000, 1958.